Supplemental Data

Supplementary methods

Mice genotyping

All the littermates were genotyped using 2 PCR primers sets: Primers A (5'-CCTTGGGGTGTGAGCCTGAT-3') and D (5'-AGCTCTCTACTTGTGACTTG-3') produced a 212 bp band from the null allele, while primers B (5'-CAGTGTCTGAGCGAGCAGAG-3') and C (5'-CATGAATTCAAGCAGGAGAGCGA-3') detected a 213 bp band in the wild-type allele. PCR amplification was run under cycling conditions of 94°C for 30 s, 58°C for 30 s, and 72°C for 30 s.

RP58 conditional mutants were obtained from crossing double heterozygous mice (*RP58*$^{fl/+}$; *Nestin-Cre*) with *RP58* homozygous floxed (*RP58*$^{fl/fl}$) mice. Six different genotypes in the littermates were assayed by 3 different PCRs: Primers A and C detected the *RP58* wild-type (389bp fragment) and floxed allele (443bp fragment), and primers A and D monitored the null allele due to the germ line leakage of the *Nestin-Cre* line (1). Primers Cre5' (5'-TAAAGATATCTCACGTACTGACGGTG-3') and Cre3' (5'-TCTCTGACC AGAGTCATCCTTAGC-3') were used to detect the *Nestin-Cre* transgene. PCR genotyping was performed on genomic DNA isolated from liver of embryos or pups, under the above conditions (2).

Supplementary Figure Legends

Supplementary Figure 1. Gene targeting strategy to generate a floxed *RP58* allele.

a) Top: Diagram of the *SpeI* genomic fragment containing the main exon, coding for the full-length RP58 (CDS box in red), and the 5' (box in yellow) and 3' UTR (box in blue) regions, and map of the targeting vector showing the *loxP* sites flanking both the *RP58* exon and flrted NEO cassette. Middle: Map of the targeted allele with the floxed exon and flrted NEO cassette. Bottom: Generation of the floxed and null alleles after Flp or Cre-mediated removal. The fragment sizes were shown in bracket corresponding to the *SpeI* fragments in four different alleles.

b) Southern blot analysis of littermates with their genotypes as noted (1 to 4). The blots were hybridized with 5' and 3' probes (location is indicated in the maps of the different alleles in a).

c) In situ hybridization and immunohistochemistry analyses of $RP58^{fl/+}$ and $RP58^{fl/-}$; *Nestin-Cre* P0 cortices confirmed the absence of *RP58* transcripts and proteins in *RP58* mutant mice. Scale bar = 200 μm.

Nestin-Cre mice also show Cre expression in the germ cells (1) and thus in our study we have used both $RP58^{fl/fl}$;*Nestin-Cre and* $RP58^{fl/-}$;*Nestin-Cre* mice as *RP58* mutant mice (*RP58* cKO). *RP58* cKO mice die at ~3 weeks of age while *RP58* KOs lacking *RP58* function ubiquitously are of early perinatal lethality, indicating additional functions of

RP58 outside the central nervous system, consistent with its expression in various tissues (not shown).

Supplementary Figure 2. *RP58* mutant cortices display a reduced thickness.

Quantification of cortical thickness in embryonic (E15.5) and postnatal (P2) control and *RP58* cKO mice (see Fig. 1g-j). Asterisks denote significant changes (p=0.0014 for E15.5, p=0.0062 for P2)

Supplementary Figure 3. *RP58* expression in the developing mouse neocortex.

a-d) *RP58* expression in the developing mouse cerebral cortex. The expression of *RP58* mRNA was analyzed by *in situ* hybridization with a digoxygenin-labeled antisense *RP58* RNA probe on frozen horizontal (a, b) and sagittal (c, d) sections of forebrain or cortex at the embryonic (E) ages noted. *RP58* is first expressed in the ventricular zone (VZ) (a), later in the cortical plate (CP) (arrow in b, c) and in the intermediate zone (IZ) (d) between the VZ and CP. Scale bars = 50 μm for a, c; 100 μm for b; 200 μm for d.

Supplementary Figure 4. *RP58* KO mice show a similar prenatal cortical phenotype as *RP58* cKO mice.

Sagittal sections of E16.5 (mid-gestation) and E19.5 (late-gestation) control and *RP58* KO cortices at low (a-b, q-r) and high (c-p, s-af) magnifications. The top two rows show Nissl staining and the rest show the results of *in situ* hybridizations with specific

digoxygenin-labeled antisense RNA probes as noted. The markers analyzed are indicated on the left. Note the complete absence of *RP58* mRNA in null mutants and the loss of upper-layer cells marked by the various genes analyzed. Arrows (n, ad) point to residual *cux2* expression in the cortical plate. Asterisk (j) indicates ectopic *ER81* expression in the VZ. Scale bars = 500 μm for a-b; 200 μm for c-p; 500 μm for q-r; 100 μm for s-af.

Supplementary Figure 5. The number of CTIP2$^+$ cells is not changed in the *RP58* mutant.

Counting of CTIP2$^+$ cells in the control or *RP58* mutant cortices did not show any significant differences.

Supplementary Figure 6. Increased apoptosis in *RP58* mutant cortices.

a, b, d, e) Sagittal sections of control and *RP58* cKO cortices at E16.5 (a, b) and P2 (d, e). Arrows point to cleaved Caspase3$^+$ cells in brown after immunohistochemistry.

c, f) Quantification of the number of cleaved Caspase3$^+$ apoptotic cells in control and *RP58* mutants at E16.5 (c) and P2 (f). Scale bars = 100μm. Asterisks denote significant changes ($p<0.05$).

Supplementary Figure 7. *RP58* mutant cortices display abnormal cell positioning.

a-f) BrdU birth-dating analyses performed at E11.5 (a, d, g), E13.5 (b, e, h) or E16.5 (c, f, i) and analyzed at P0 (a, d, g) or P2 (b, c, e, f, h, i). Postmitotic BrdU$^+$ cells acquire

characteristic positions in the neocortex after migration, as seen in control brains (a-c). Similar analyses reveal the abnormal positioning of BrdU-labelled cells in *RP58*-mutant brains (d, e, f). All panels show BrdU immunohistochemistry (brown) and *in situ* hybridization for c*tgf* (blue, clearly visible in the subplate just below the lower boundary of the deep region; a-c).

g-i) Quantification of BrdU-labeled cells in upper, middle or deep bins as shown in (a-f) for control and *RP58* cKO brains. Due to differences in cortical thickness between the mutant and control brain, quantification was performed by counting $BrdU^+$ cells from the subplate and above. The subplate is vizualised with *ctgf* expression and although *ctgf* expression is highly reduced in the mutant, the presence of few expressing cells allowed to locate the subplate in the mutant cortex. The region between the pial surface and the subplate was then divided in 3 equal bins (upper, middle and deep). Only strong $BrdU^+$ cells were counted on 3 sections/brain from 3 brains of control or mutant mice.

j-m) Same magnification views of sections of control and *RP58* cKO cortices showing the abnormal positioning of $BrdU^+$ cells, born at E11.5 and analyzed at E15.5. The left column show Nissl-staining of adjacent sections to those shown on the right column. Note the preplate splitting in the control (arrows in k), while most of the cells labeled at E11.5 are localized close to the pial surface in the *RP58* mutant (arrow in m).

n-q) Abnormal location of $CSPG^+$ (Chondroitin Sulfate ProteoGlycans) (n, o) and $Tbr1^+$ (p, q) cells in *RP58* mutant cortices (o, q) as compared with control siblings (n, p), revealing the absence of a preplate splitting in the *RP58* mutant.

Scale bars = 100 μm for a-f, j-o; 200 μm for p-q.

Supplementary Figure 8. *RP58* is required for cortical neurogenesis.

a) Western blot analyses of the MAP2 levels in E14.5 wild-type and *RP58* KO cortices. Note that MAP2 levels are already decreased at this early stage.

b) Western blot analyses of the levels of cell type-specific markers in E18.5 wild-type and *RP58* KO cortices. RP58 is lost in the mutant cortices, which have increased Nestin, GFAP and cleaved Caspase 3 levels and decreased MAP2 levels. Tubulin is shown as loading control.

c) Sagittal sections of P2 control and *RP58* cKO cortices showing the reduction of NeuN expressing cells in the mutant brain. Scale bar =100μm.

Supplementary Figure 9. *RP58* mutants show a decrease in proliferating cortical cells outside the ventricular zone.

Quantification of the number of phospho-Histone $H3^+$ ($PH3^+$) cells per arbitrary area (at least 3 sections/E16.5 embryo, 3 embryos/genotype) as shown in the ventricular zone (VZ) vs. outside the ventricular zone (SVZ) in control and cKO cortices. A Wilcoxon two samples test was applied for statistical analysis ($p<0.0005$ for SVZ).

Supplementary Figure 10. The three cell subpopulations in *RP58* mutant cortices are comparable to those in control cortices in terms of basic molecular identity.

a) Characterization of the three cell populations described in Fig. 4a by the expression of key molecular markers of RGC (*blbp, glast, pax6*), INP (*tbr2*) and neurons (*tbr1, MAP2*) in the *RP58* KO.

b) Analyses of the expression levels of the proliferation marker Ki67 in A, B and C populations. Note that the levels of Ki67 expression in the mutant C cells are low and similar to the C cells isolated from control cortices. This result indicates that the C cells both in the control and in the *RP58* mutant are not actively cycling.

Supplementary Figure 11. Conserved RP58 binding sites on the *ngn2* and *neuroD1* genomic regions.

The sequences of two binding sites in the *ngn2* promoter region are highly conserved between mouse and human: BS1 is completely identical for 12 nucleotides between the two species while BS2 has 8 identical nucleotides out of 12 (3 of the different nucleotides are in the core binding site). Note that nucleotide differences between mouse and human are indicated in black. The BS in the *neuroD1* promoter region is also conserved during evolution as the mouse and human sequences share 9 identical nucleotides in 12 (all nucleotides in the core binding site are identical).

Supplementary Figure 12. RP58 is recruited at the *ngn2* promoter region containing BS1, another putative RP58 binding site.

a) Schematic diagram showing the localization of the primers used in the ChIP-PCR in panel (b). The *ngn2* gene is indicated by green boxes. The putative RP58 binding sites (BS1 and BS2) in the 5' *ngn2* genomic region are indicated by red boxes.

b) Chromatin immunoprecipitation (ChIP) analyses of RP58 recruitment in control and *RP58* KO cortices using primers specific to the *ngn2* genomic region encompassing the RP58 binding site BS1 at chr3: 127335761-127335928 (168bp). Note that the histogram shows the fold enrichment of WT/KO.

Supplementary Figure 13. **RP58 is specifically recruited to the *ngn2* and *neuroD1* promoter.**

The recruitment of RP58 on *ngn2* and *neuroD1* promoter and a control genomic region (chr11:69532882-69533025) in wild type cortices relative to non-specific IgG control, as measured by ChIP-PCR experiments.

Supplementary Figure 14. *Ngn2* is ectopically expressed in the *RP58* mutant developing cortical plate.

Sagittal sections of E16.5 WT (control) and mutant (*RP58* cKO) cortices showing the results of *in situ* hybridizations with specific digoxygenin-labeled antisense RNA probes

as noted. The markers analyzed are indicated on the left. Note the complete absence of *RP58* mRNA in mutants and the ectopic *ngn2* expression (arrow) in the mutant cortical plate, the region containing the sorted C cell population (Figure 4). Scale bar = 200 μm.

Supplementary References

1. Chen RZ, Akbarian S, Tudor M, Jaenisch R. Deficiency of methyl-CpG binding protein-2 in CNS neurons results in a Rett-like phenotype in mice. *Nat Genet* 2001; **27:** 327-331.

2. Leneuve P, Zaoui R, Monget P, Le Bouc Y, Holzenberger M. Genotyping of Cre-lox mice and detection of tissue-specific recombination by multiplex PCR. *BioTechniques* 2001; **31:** 1156-1160, 1162.

3. Aoki K, Meng G, Suzuki K, Takashi T, Kameoka Y, Nakahara K*, et al.* RP58 associates with condensed chromatin and mediates a sequence-specific transcriptional repression. *J Biol Chem* 1998; **273:** 26698-26704.

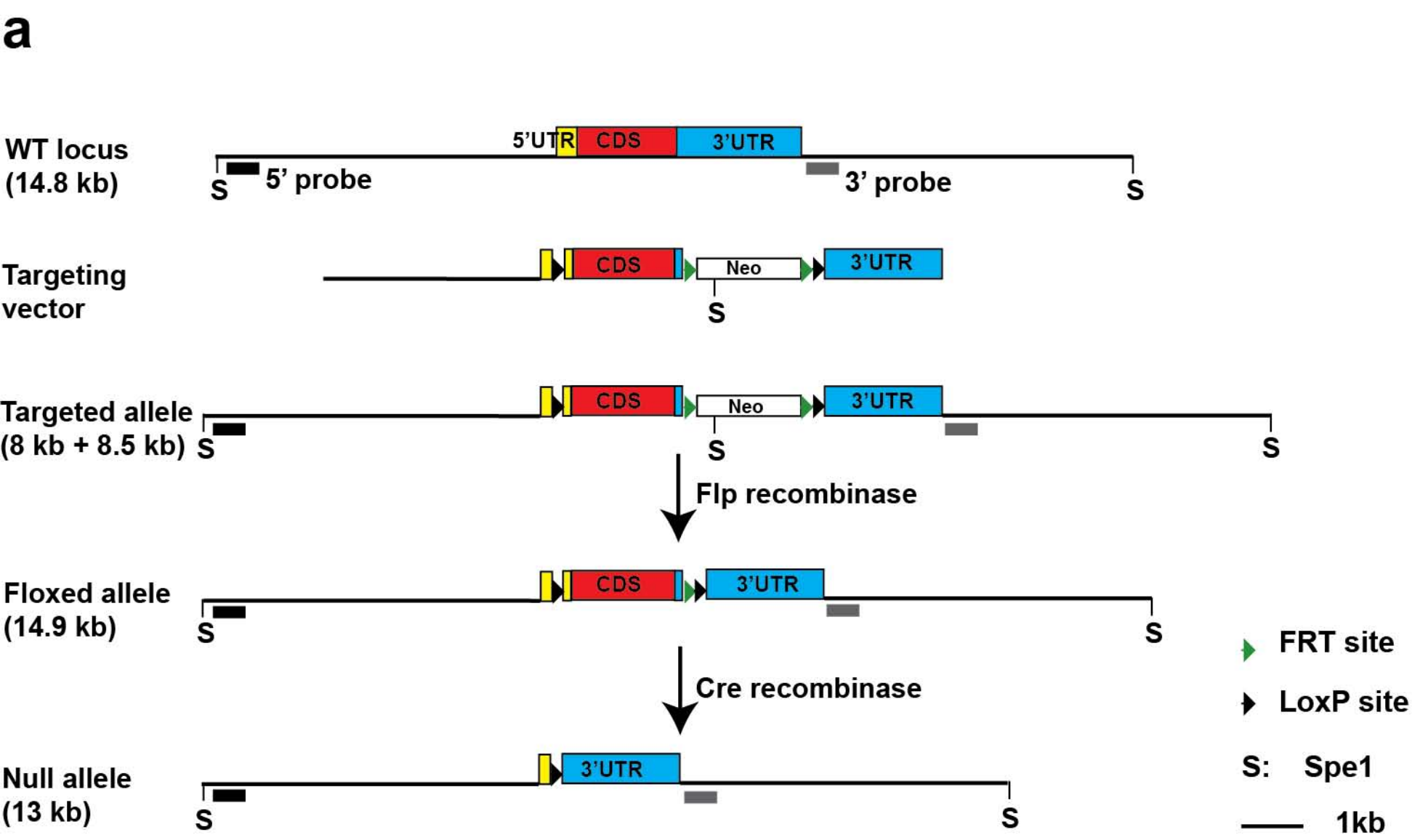

C Xiang et al.

Supplementary Figure 1a

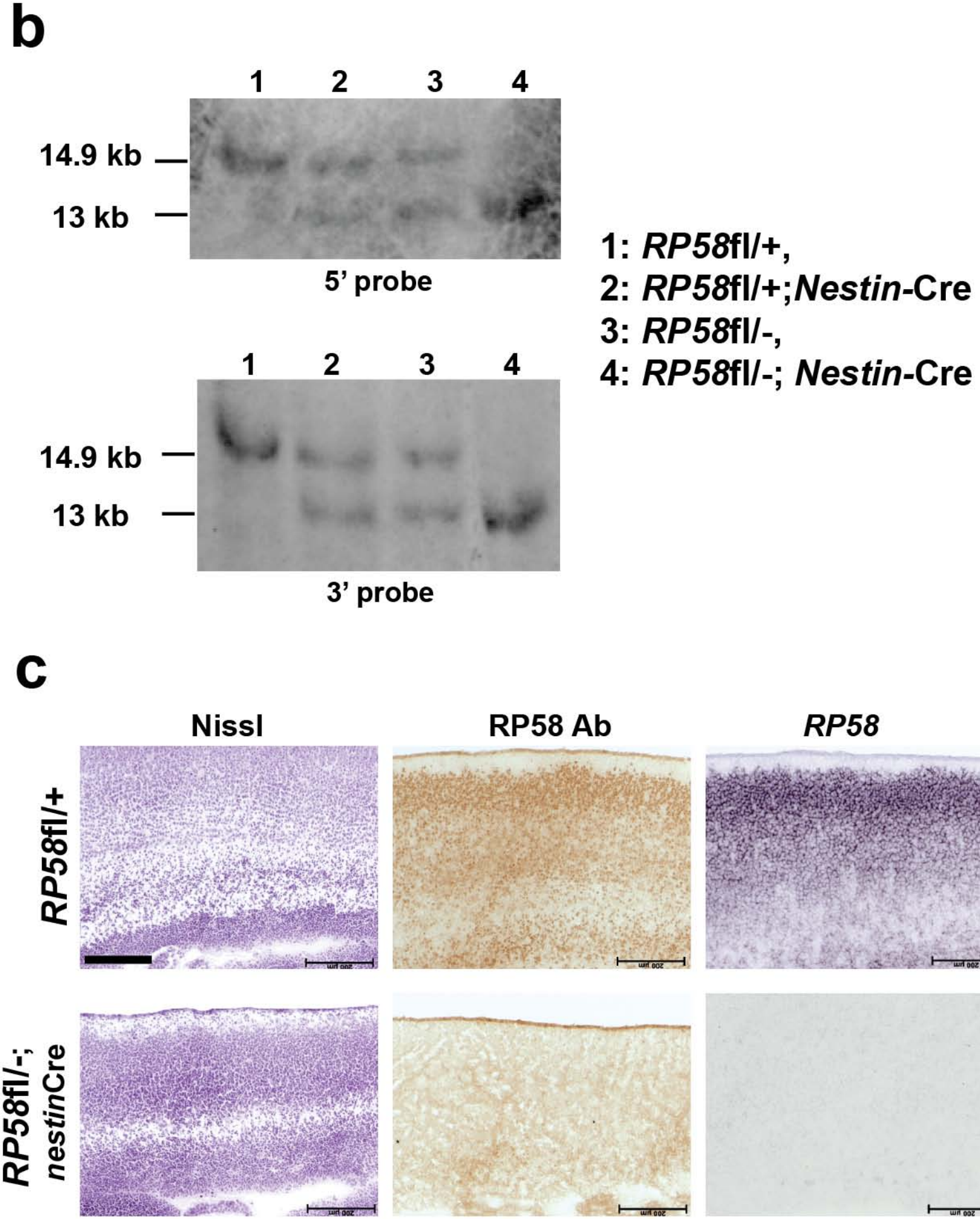

C Xiang et al.

Supplementary Figure 1b-c

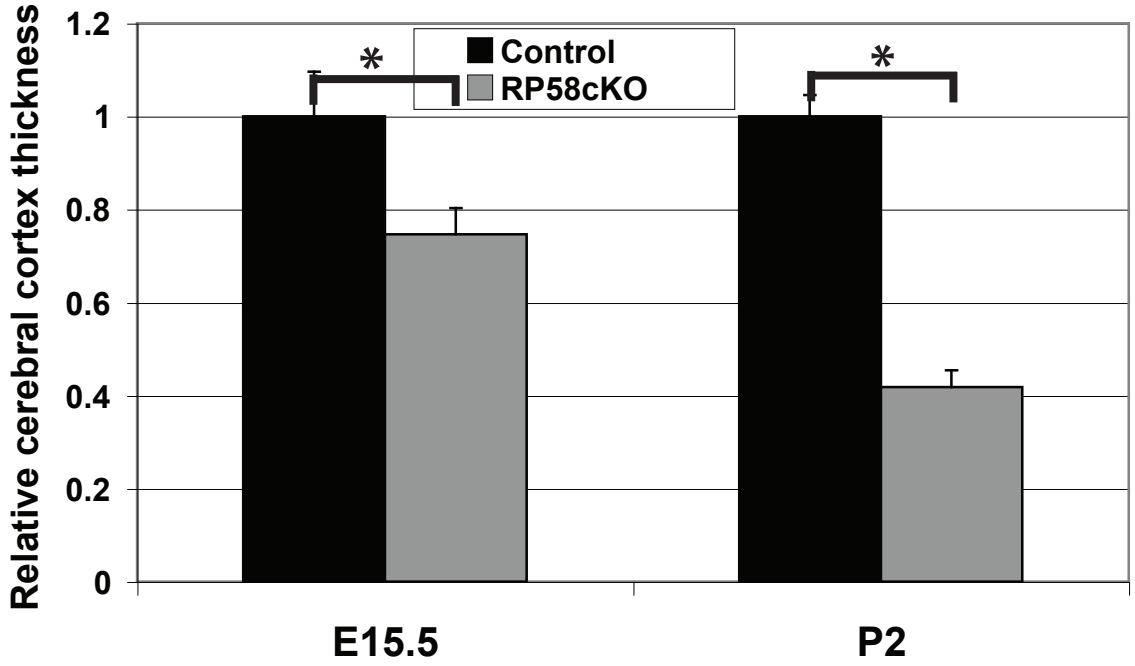

Supplementary Figure 2

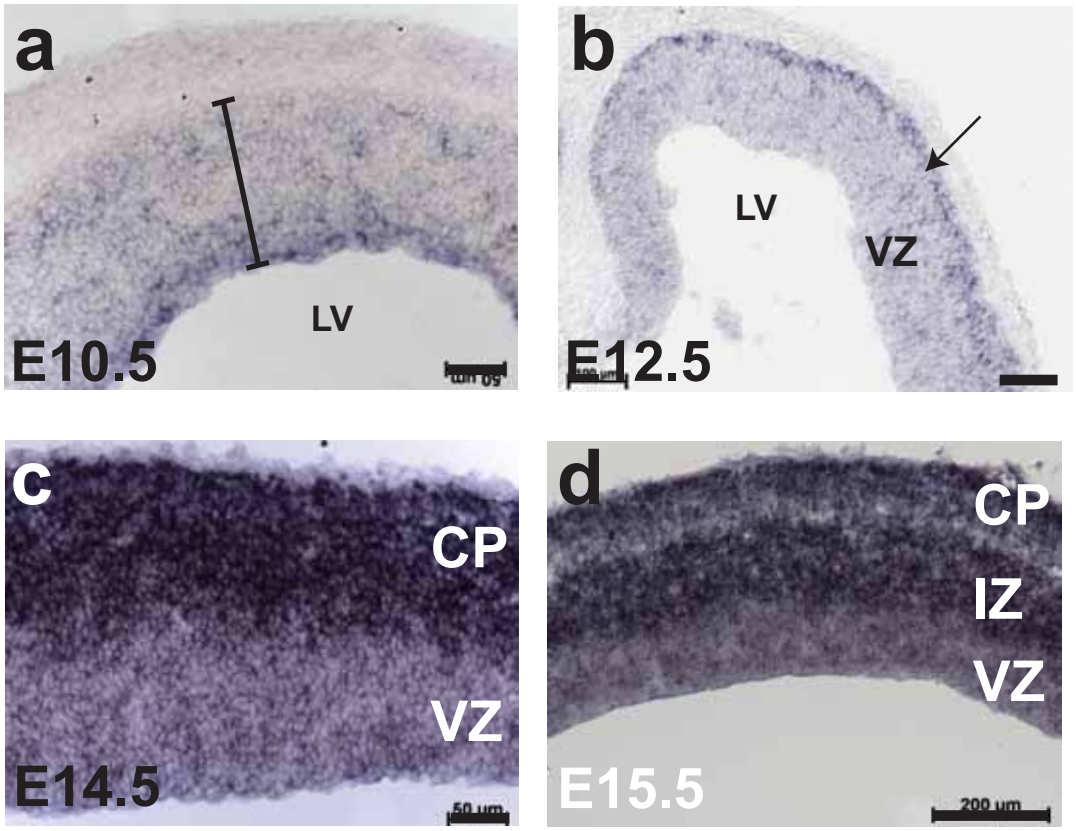

Supplementary Figure 3

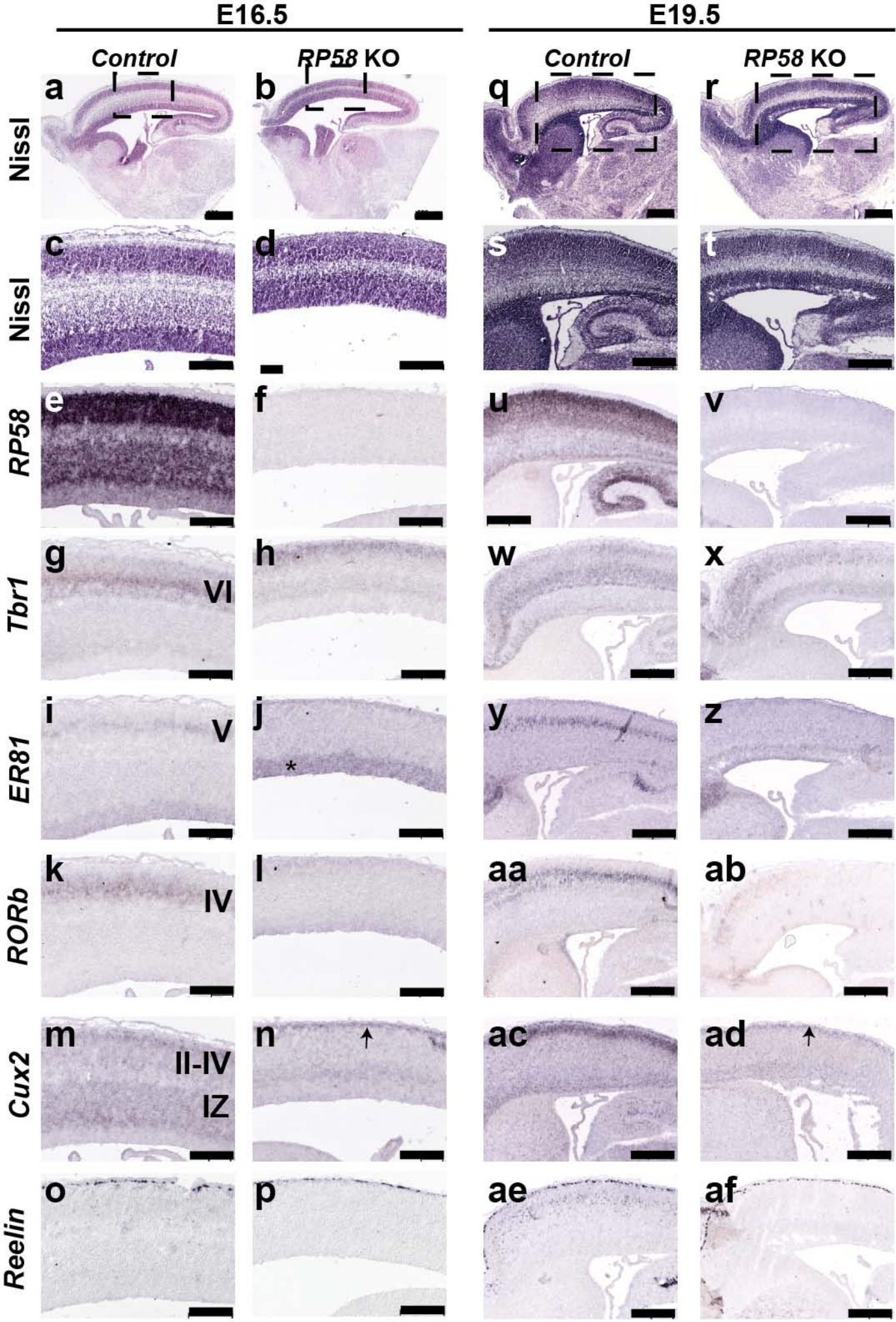

C Xiang et al.

Supplementary Figure 4

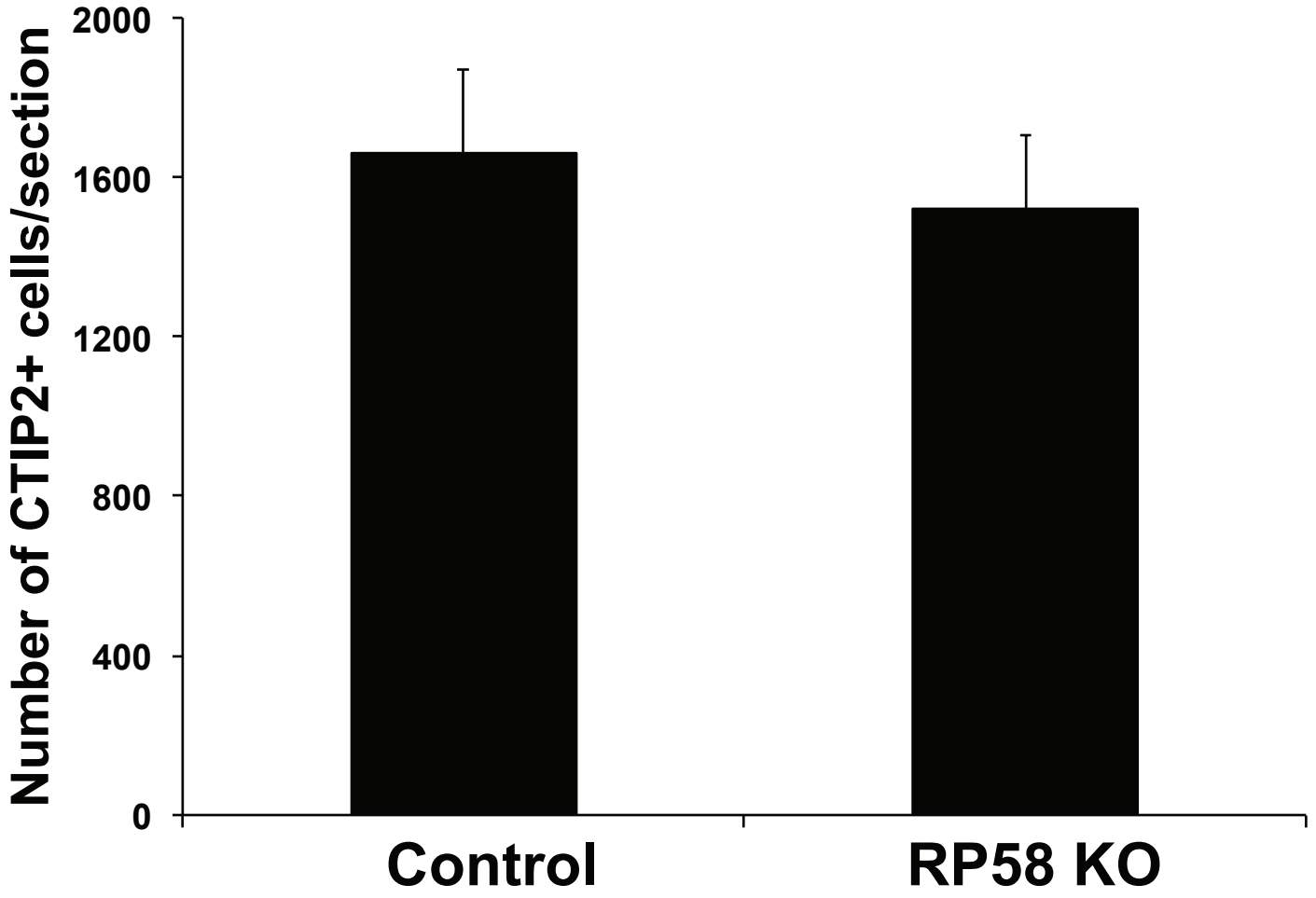

Supplementary Figure 5

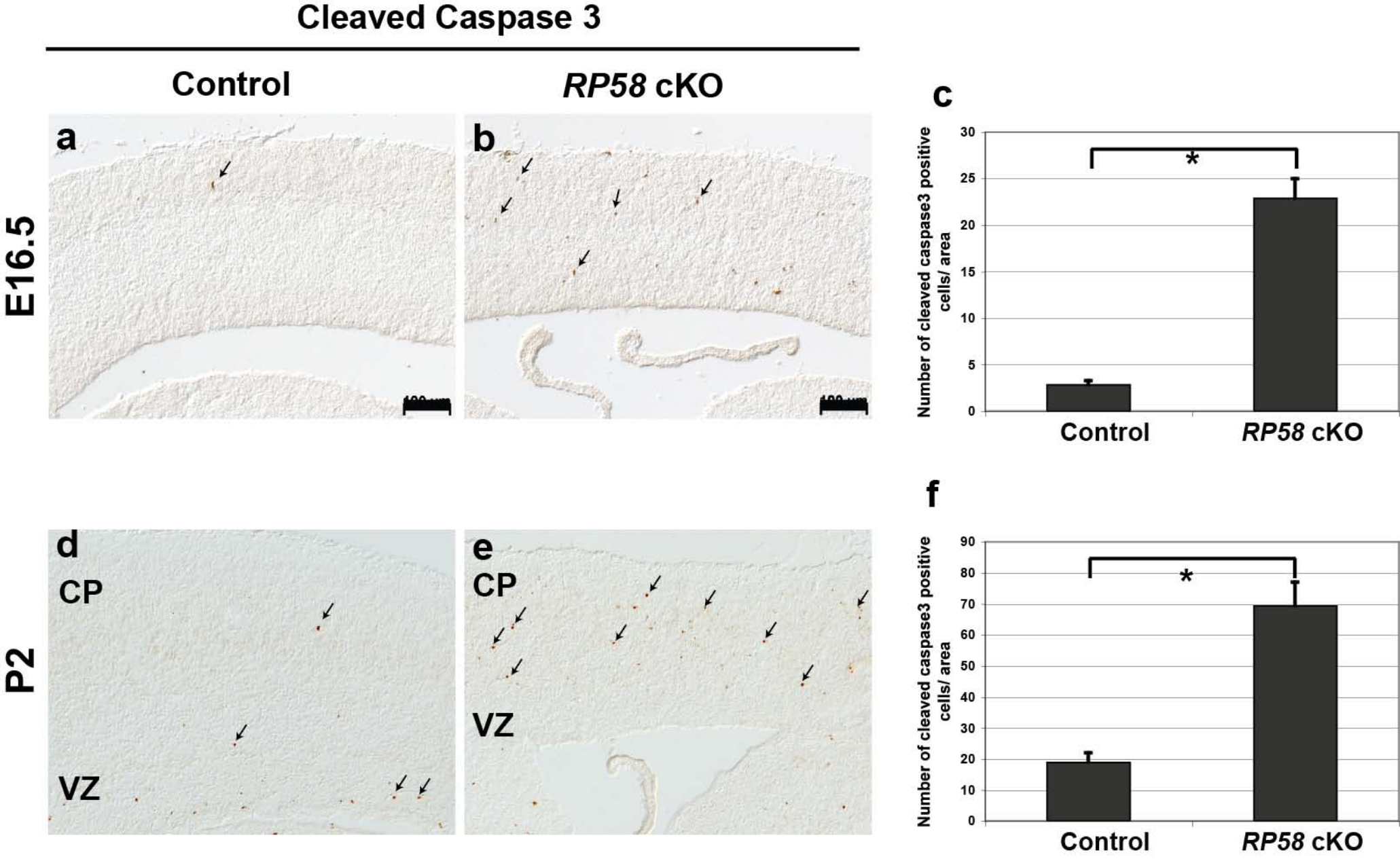

C Xiang et al.

Supplementary figure 6

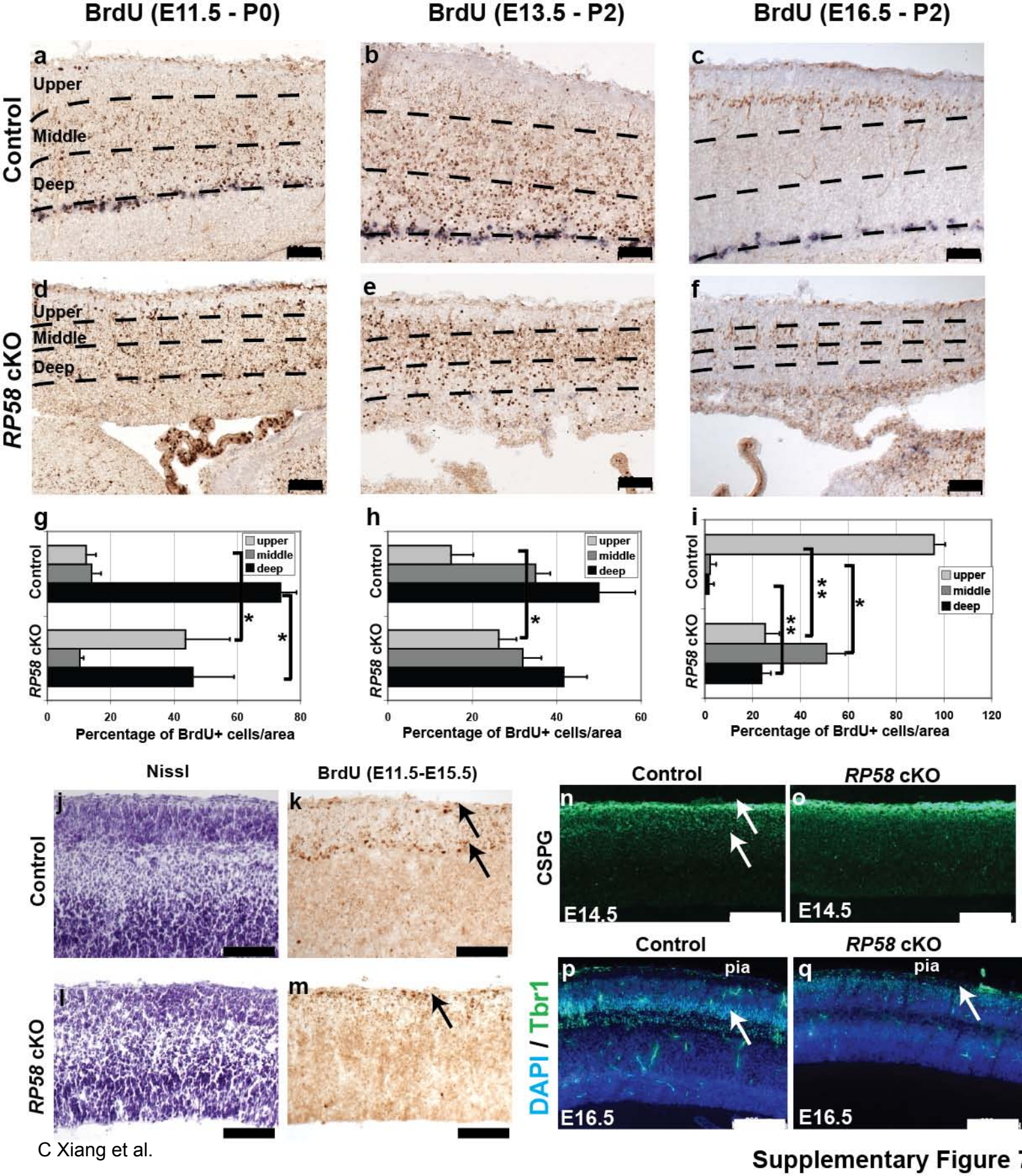

C Xiang et al.

Supplementary Figure 7

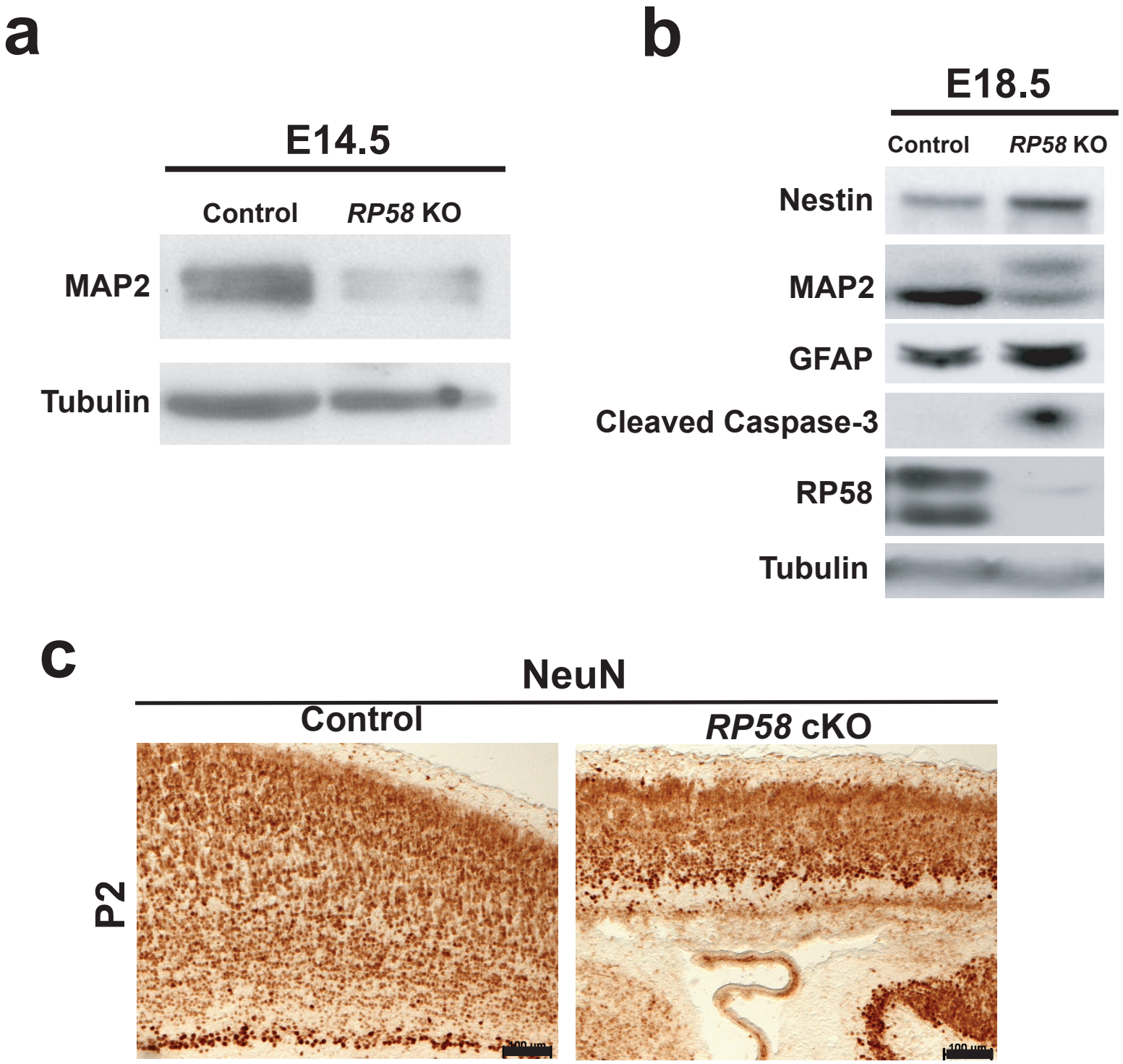

Supplementary Figure 8

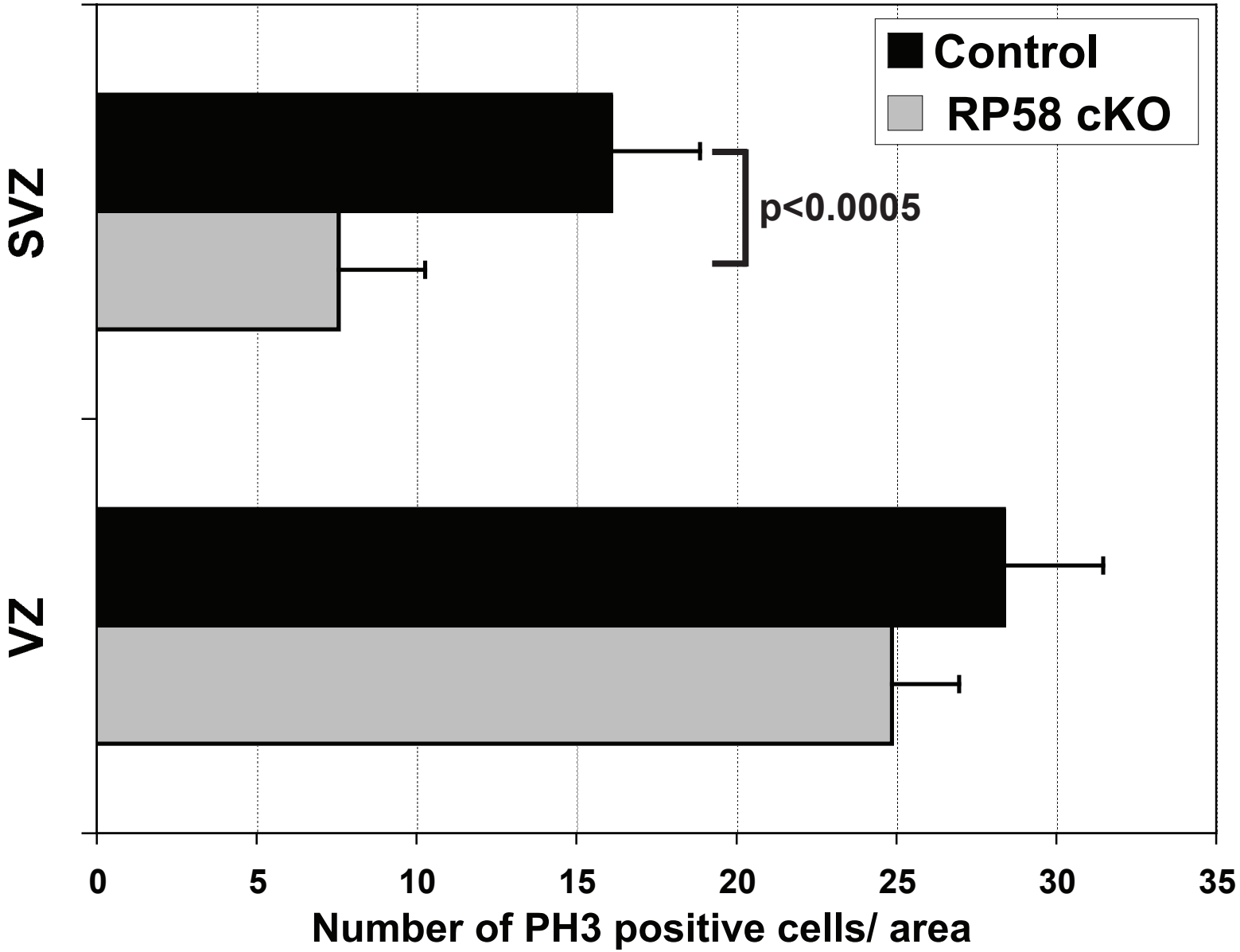

Supplementary Figure 9

C Xiang et al.

a

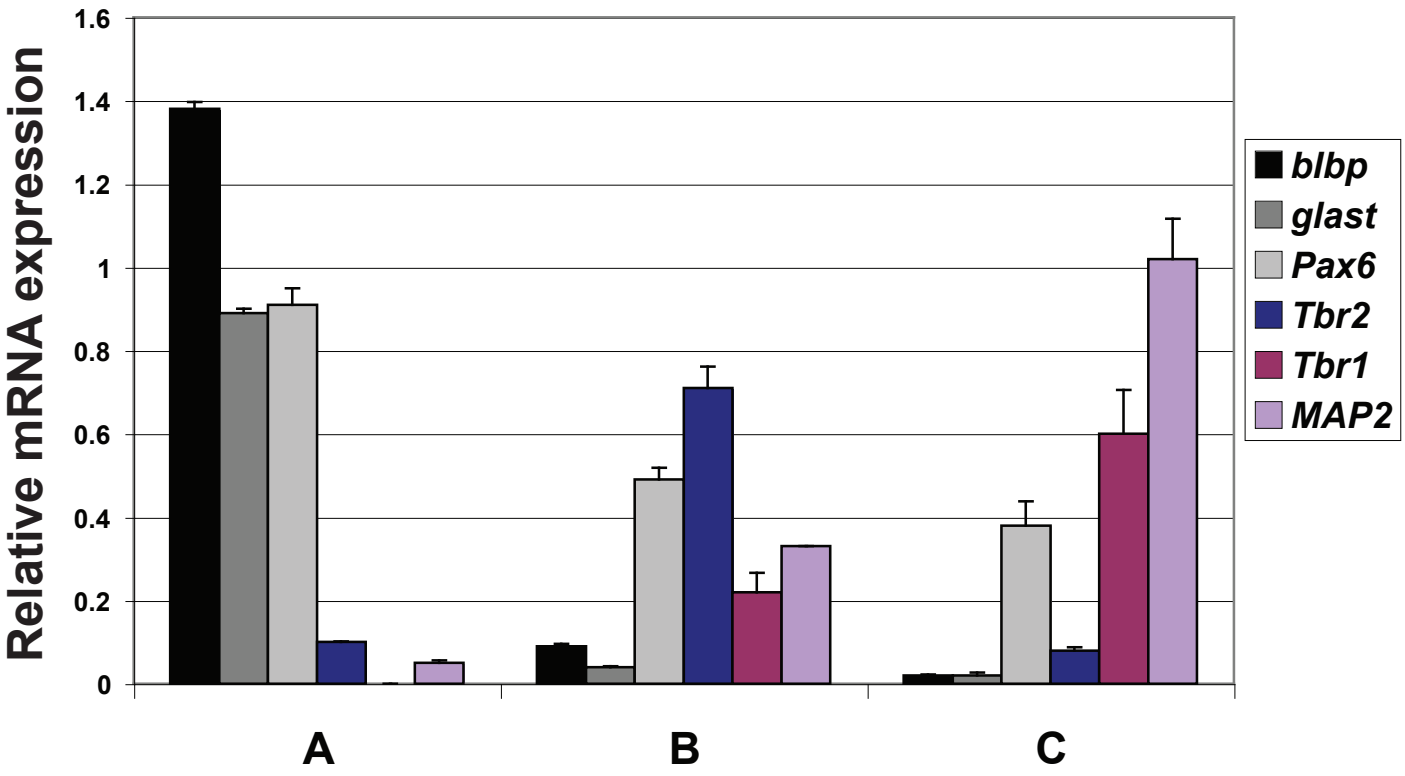

b

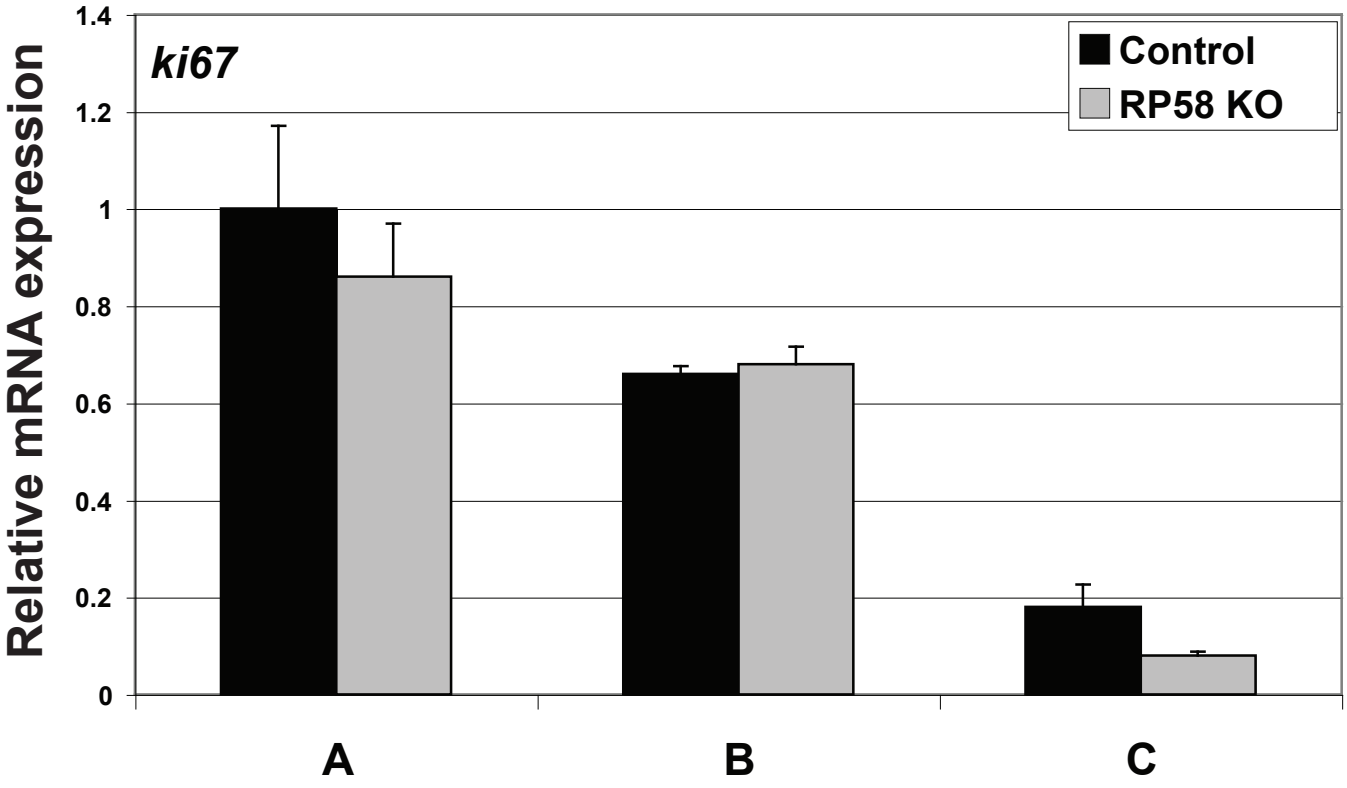

Supplementary Figure 10

Mouse *ngn2*-BS1:	CCCTCCCCTGGC
Human *ngn2*-BS1	CCCTCCCCTGGC
Mouse *ngn2*-BS2:	GACACATCTGGA
Human *ngn2*-BS2:	GGCACAGTTAGA
Mouse *neurod1*-BS:	ACCTCATCTGGA
Human *neurod1*-BS:	GCTTCATCTGTA

Supplementary Figure 11

a

b

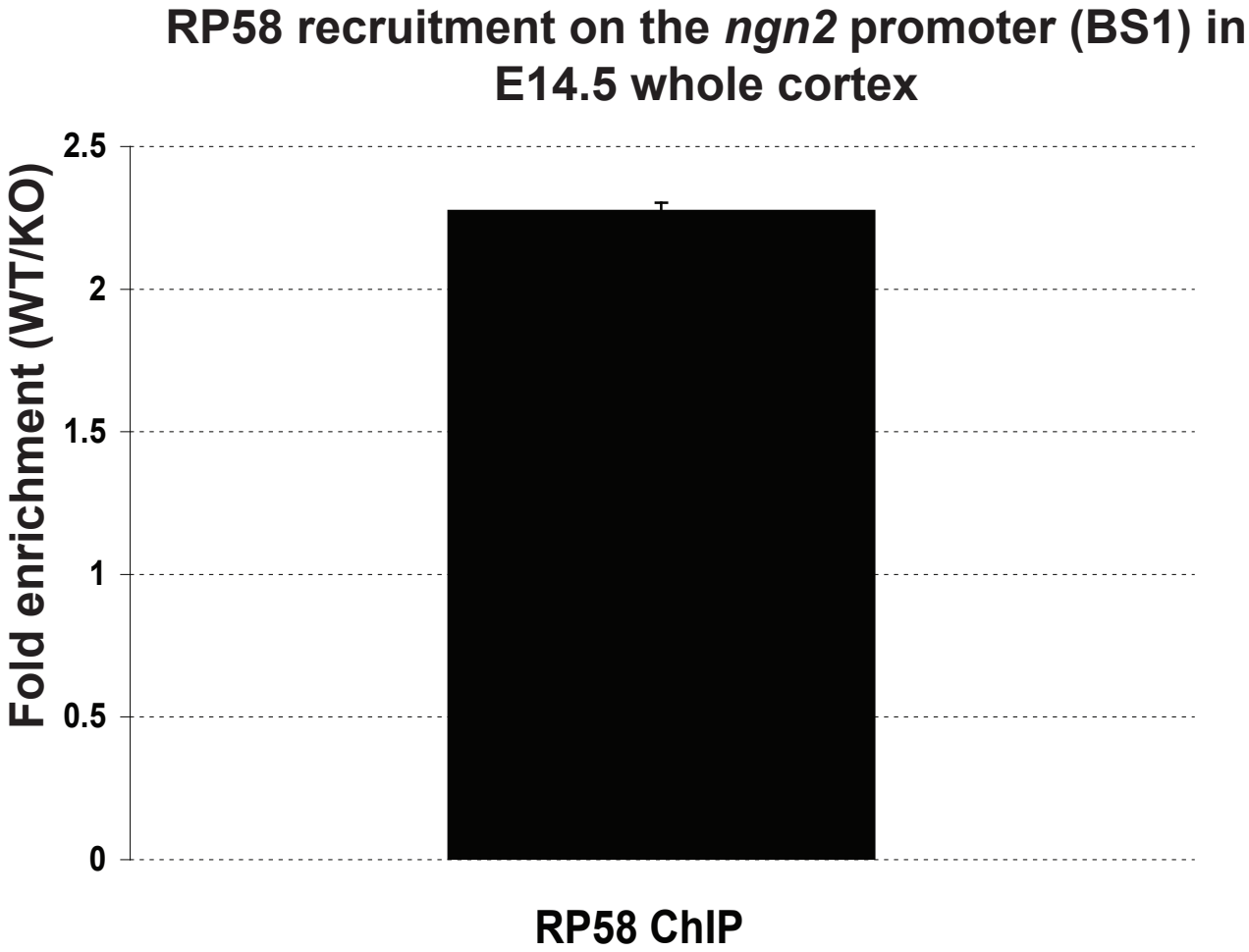

Supplementary Figure 12

C Xiang et al.

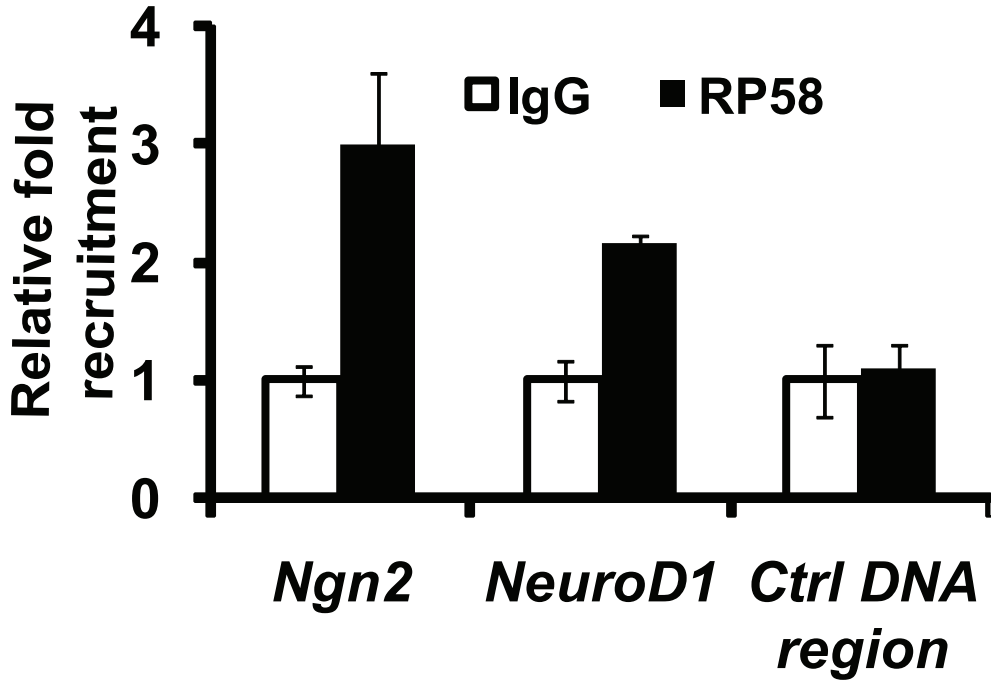

Supplementary Figure 13

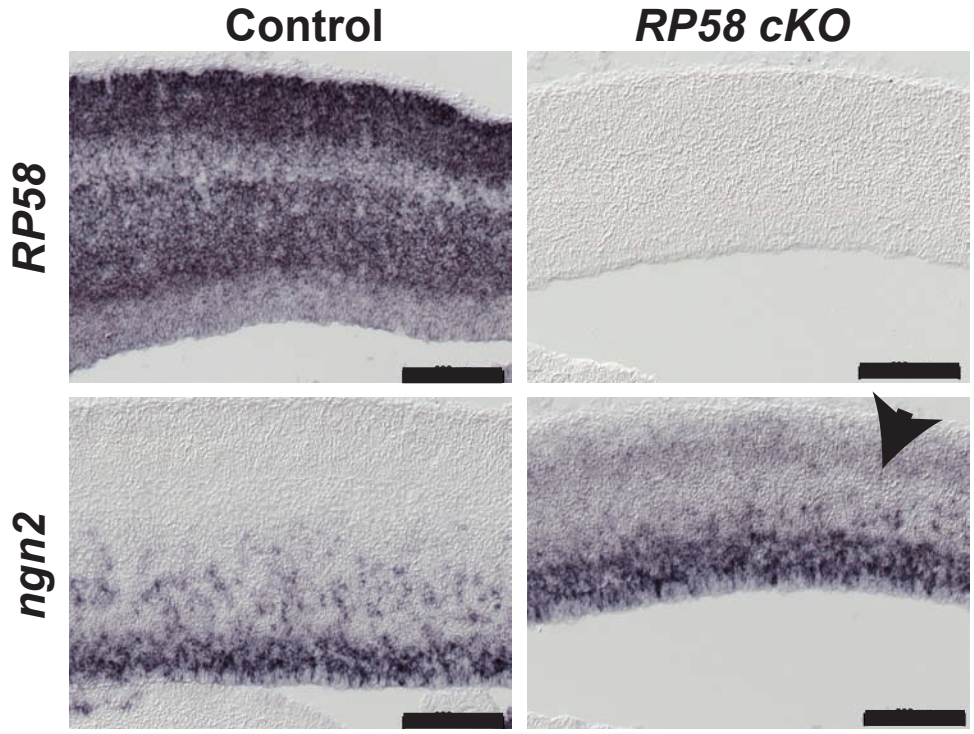

Supplementary Figure 14